



Cite this: *Mol. Syst. Des. Eng.*, 2018, 3, 408

## Use of ionic liquids to remove harmful $M^{2+}$ contaminants from hydrocarbon streams†

Paul J. Corbett,<sup>a</sup> Alastair J. S. McIntosh,<sup>a</sup> <sup>a</sup> Michael Gee<sup>b</sup> and Jason P. Hallett <sup>\*a</sup>

Zinc contaminants have been identified as suspects leading to nozzle deposit formation and copper contaminants quickly reduce the oxidation stability of diesel fuel. Ionic liquids (ILs) are commonly referred to as ‘designer solvents’ due to the great degree of fine-tuning of physical and chemical properties afforded by modification of the constituent cation and anion. The tunable properties of the IL ions allows the ‘design’ to meet the requirements for a particular application, making ILs an ideal potential candidate for the extraction of trace (ppb to ppm) amounts of zinc and copper heavy metals from diesel fuel. We report for the first time that ILs can extract up to 99.3% of zinc at a zinc concentration of just 2 mg kg<sup>-1</sup> and copper can be extracted up to 99.7% at copper concentration of just 1 mg kg<sup>-1</sup> from a model diesel fuel. Factors affecting the extent of extraction were investigated *via* correlation with experimental descriptors. <sup>23</sup>Na NMR was used in the determination of donor number (DN) and Kamlet–Taft parameters were gathered for each IL providing information of possible hydrogen-bond acidity/basicity ( $\alpha/\beta$ ), and dipolarity/polarizability effects ( $\pi^*$ ). In addition, the non-random two liquid (NRTL) model was applied to determine  $\tau$  parameters for each of the ILs. We determined that the extraction is controlled strongly by the hydrogen bond basicity of the IL which is directly related to the ability of the anion of the IL to complex Zn<sup>2+</sup> and Cu<sup>2+</sup> thus removing it from the fuel. DN,  $\tau$  parameters and  $\beta$ , in addition to density and viscosity values, provide further information on the extraction mechanisms and predict performance, informing chemical design of ILs that are ideal for fuel purification.

Received 1st October 2017,  
Accepted 6th February 2018

DOI: 10.1039/c7me00111h

rsc.li/molecular-engineering

### Design, System, Application

In this research we utilized solvent characteristics to design ionic liquids for the extraction of trace metal impurities from diesel fuel. Because of the application, we gave preference to innocuous elements in fuels (CHO and minimal N). We also used solvation parameters, including Kamlet–Taft polarity and hydrogen bonding parameters, to estimate extraction with a focus on Gutmann donor number (for donation to the metal center) and indications of chelating ability for divalent metals. We also correlated these parameters with a variety of physical properties to establish engineering design criteria related to performance. While diesel fuel purification at the ppm level is our present target, this has the potential to establish a generic platform for trace metal removals with ionic liquids.

## Introduction

In recent years, great improvements in the design of diesel engines have been achieved particularly by advances in diesel injection (DI). A decrease in the diameter of the nozzle orifice to enhance spray characteristics has led to increased spray pressures enabling high power densities and decreased emissions.<sup>1</sup> However, this leaves injectors vulnerable to the forma-

tion of nozzle deposits.<sup>2</sup> Zinc can contaminate diesel fuels *via* contact with lubricants or surfaces containing Zn. It then acts as a catalyst in the formation of carbon deposits which induce nozzle deposit formation.<sup>3</sup> The deposits tend to form in the spray holes, blocking partially, or completely hindering, the smooth delivery of a fuel injection. These deposits can lead to rough idling, power loss, and high emissions.<sup>4</sup> Copper contamination has been shown to significantly reduce the oxidative stability of the diesel fuel, determined *via* the Rancimat oxidative stability test.<sup>3</sup> Ionic liquids are proving to be solvents of ever greater interest and utility.<sup>5</sup> They have been the subject of widespread academic study in recent years and have already found use in many applications.<sup>6–10</sup> Exploiting the advantageous solvent properties of ionic liquids could prove very beneficial to the energy industry. As a

<sup>a</sup> Department of Chemical Engineering, Imperial College London, South Kensington, London, SW7 2AZ, UK. E-mail: j.hallett@imperial.ac.uk

<sup>b</sup> Shell International Limited, 40 Bank Street, Canary Wharf, London, E14 5NR, UK

† Electronic supplementary information (ESI) available: See DOI: 10.1039/c7me00111h

result of their ionic character, ILs have negligible vapour pressure under standard process operating conditions, thus rendering them easily recoverable from molecular volatile compounds and avoiding losses to the atmosphere; benefiting the environment. Moreover, a judicious selection of their constituent ions can tune the properties of the ionic liquids to a considerable extent, thus allowing the 'design' of the ionic liquid to meet the requirements for a particular application *i.e.* task-specific ionic liquids.<sup>11</sup> ILs could be utilised here to extract both Zn<sup>2+</sup> and Cu<sup>2+</sup> from diesel fuel and thus prevent deposit formation and restore the oxidative stability of the fuel. Limited research has been conducted on extractions using ionic liquids with diesel fuels outside of desulfurization/denitrogenation. We believe we present the first study on the extraction of contaminant Zn<sup>2+</sup> and Cu<sup>2+</sup> from model diesel fuels using ionic liquids, providing a pathway for future uses of ionic liquids in the biphasic extraction of metal impurities. A related manuscript considering the removal of Na<sup>+</sup> in a similar manner is available.<sup>12</sup>

### Ionic liquid selection

A wide range of ionic liquids were synthesised (Fig. 1) to determine which cationic and anionic components of ILs are desirable for the extraction of Zn<sup>2+</sup> and Cu<sup>2+</sup> from *n*-hexadecane. Imidazolium (with butyl or octyl alkyl chains) and pyrrolidinium (with butyl alkyl chains) based ILs were selected due to their varying cationic properties (individual ring structures) and alkyl chain lengths which gives variety without the incorporation of additional functional groups. Specific to these structures, the imidazolium cation provides a delocalized charged ring whereas the pyrrolidinium cation

provides a charged atom. The anions in this study were employed for a number of reasons in addition to being thought of as good candidates to chelate M<sup>2+</sup> ions:

1. The [N(Tf)<sub>2</sub>]<sup>-</sup> and [OTf]<sup>-</sup> anions were selected due to their wide use; thus there is a vast amount of physical property data available.
2. The [OAc]<sup>-</sup> anion was selected as it contains only atoms of CHNO which is most appealing for a fuel application.
3. The [Me<sub>2</sub>PO<sub>4</sub>]<sup>-</sup> and [Me<sub>2</sub>SO<sub>4</sub>]<sup>-</sup> anions were selected to provide information on whether a sulfur or phosphorus centre is preferable in the chelation of M<sup>2+</sup> ions.
4. The [HSO<sub>4</sub>]<sup>-</sup> anion was selected to determine if H-bonding played a major role in chelation.
5. The chloride (Cl<sup>-</sup>) anion was selected to examine possible formation of a precipitate within the extraction and to determine how this could affect the results.
6. Finally, the dithiocarbamate (DTC) anion [S<sub>2</sub>CN(C<sub>2</sub>H<sub>5</sub>)<sub>2</sub>]<sup>-</sup> was selected as it possesses an excellent ability to form metal complexes. DTCs have displayed the ability to form stable complexes with every transition metal in the periodic table<sup>13</sup> which originates from the flexible electronic nature of DTCs; the sulfur atoms possess σ-donor, and π-back-donation, characteristics of equal magnitude. Furthermore, the planar delocalised π-orbital system also enables additional π-electron flow from the nitrogen to sulfur.<sup>14</sup>

## Experimental

### Materials and methods

All chemicals and solvents used were reagent grade and employed without further purification unless noted

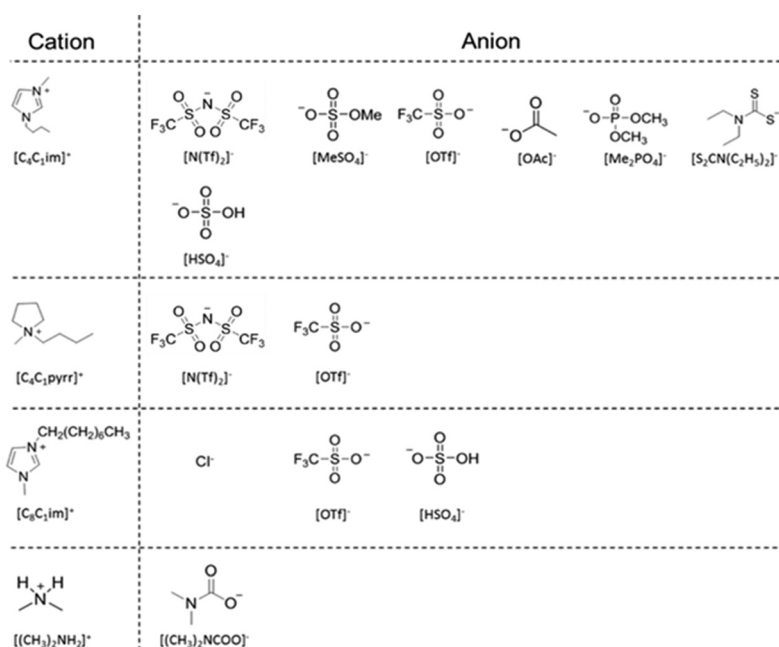


**Fig. 1** Range of ILs synthesised for use in this study 1) [C<sub>4</sub>C<sub>1</sub>im][N(Tf)<sub>2</sub>], 2) [C<sub>4</sub>C<sub>1</sub>im][MeSO<sub>4</sub>], 3) [C<sub>4</sub>C<sub>1</sub>im][OTf], 4) [C<sub>4</sub>C<sub>1</sub>im][OAc], 5) [C<sub>4</sub>C<sub>1</sub>im][Me<sub>2</sub>PO<sub>4</sub>], 6) [C<sub>4</sub>C<sub>1</sub>im][S<sub>2</sub>CN(C<sub>2</sub>H<sub>5</sub>)<sub>2</sub>], 7) [C<sub>4</sub>C<sub>1</sub>pyrr][N(Tf)<sub>2</sub>], 8) [C<sub>4</sub>C<sub>1</sub>pyrr][OTf], 9) [C<sub>8</sub>C<sub>1</sub>im]Cl, 10) [C<sub>8</sub>C<sub>1</sub>im][HSO<sub>4</sub>], 11) [C<sub>8</sub>C<sub>1</sub>im][HSO<sub>4</sub>], 12) [(CH<sub>3</sub>)<sub>2</sub>NH<sub>2</sub>][(CH<sub>3</sub>)<sub>2</sub>NCOO].

otherwise. Aqueous solutions were prepared using deionised water. The ionic liquids synthesised within this work are displayed in Fig. 1. All ILs were prepared in our laboratory from commercial starting materials, pursuing the highest purity possible in each step. The synthesis and characterisation of ionic liquids 1–11 is stated in the ESI.†

In order to gain an insight into the behaviour of ionic liquids with market fuels, synthetic models of diesel were prepared and used in the study of zinc and copper extraction. Hexadecane (99%), zinc neodecanoate ( $2 \text{ mg kg}^{-1}$ ) and copper acetylacetonate ( $1 \text{ mg kg}^{-1}$ ) were combined respectively to produce the model  $\text{Zn}^{2+}/\text{Cu}^{2+}$  contaminated diesel fuels following industry standards.<sup>3</sup>

### Extraction experiments

The extraction experiments were performed for each IL by contacting 1 mL of the ionic liquid with varying volumes of the model fuel at a uniform concentration for 1 min on a Heidolph Multi Reax Vortex Shaker and then leaving overnight to phase separate and settle. Two millilitres of the fuel phase was then transferred to a centrifuge tube and contacted with 2 mL of a 4 M  $\text{HNO}_3(\text{aq})$  solution for 1 min on the shaker. This was also left to settle overnight and 1 mL of the acid ( $\text{HNO}_3$ ) phase was then transferred to a centrifuge tube and diluted with 3 mL of distilled water to produce a 1 M solution.

Inductively coupled plasma spectrometric excitation sources have been in use since the mid-1960s,<sup>15</sup> and since then they have evolved dramatically. Inductively coupled plasma optical emission spectrometry (ICP-OES) can be used in the determination of most of the elements, the detection limits are very low usually ranging between  $1\text{--}100 \mu\text{g L}^{-1}$ .<sup>16</sup> The concentration of zinc and copper ions was determined for each sample *via* ICP-OES after performing a calibration and background check for each of the expected ions. To ensure that the data was reliable five data points were repeated at each IL to fuel volume ratio (1:20, 1:40, 1:60, 1:80 and 1:100). The distribution coefficients of these extractions were then calculated and measurements were repeated three times, and the standard deviation taken to provide error bars (Fig. 2–6). All extractions were run and left overnight in a temperature regulated room at  $22 \text{ }^\circ\text{C}$ .

### Donor number measurements

The ILs were dried *in vacuo* overnight prior to the measurements and were stored in J. Young valve NMR tubes. The probe substances (sodium trifluoromethanesulfonimide,  $\text{Na}(\text{NTf}_2)$ , and sodium trifluoromethanesulfonate,  $\text{NaOTf}$ ) were added to the IL under an inert atmosphere to give 0.2 M solutions. The samples were then sonicated at  $30 \text{ }^\circ\text{C}$  to ensure all of the sodium compounds dissolved into the ionic liquid. The chemical shift of the samples were measured at 298 K on a Bruker 400 AVANCE III HD spectrometer running TopSpin 3.2 and equipped with a z-gradient bbo/5 mm tuneable SmartProbe™.

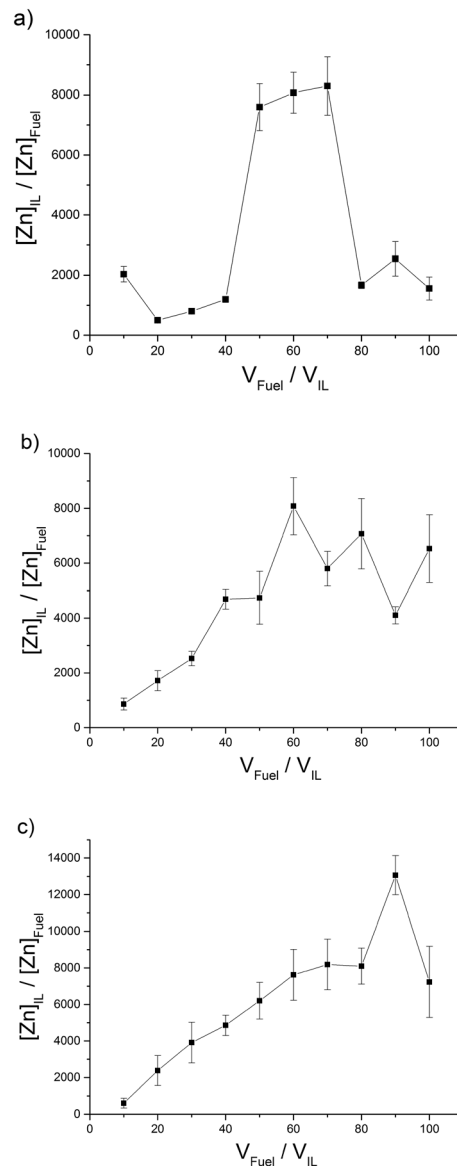


Fig. 2 ILs with high distribution (H) of  $\text{Zn}^{2+}$  into the IL phase; (a)  $[\text{C}_4\text{C}_1\text{im}][\text{Me}_2\text{PO}_4]$  (b)  $[\text{C}_4\text{C}_1\text{im}][\text{S}_2\text{CN}(\text{C}_2\text{H}_5)_2]$  (c)  $[\text{C}_4\text{C}_1\text{im}][\text{OAc}]$ .

$^{23}\text{Na}$  spectra were acquired at a frequency of 105.82 MHz using a spectral width of 21 307 Hz ( $\sim 200$  ppm centred at 0.0 ppm) and 8192 data points giving an acquisition time of 0.192 s. A deuterium lock was provided *via* a  $\text{DMSO-}d_6$  capillary tube insert. The Bruker pulse programme *zg* (*i.e.* a  $90^\circ$  pulse) and relaxation delay of 0.1 s were used. The data was processed using 8192 data points and an exponential window function of 50 Hz. Chemical shift calibration was achieved by employing a secondary reference of a saturated  $\text{NaCl}/\text{H}_2\text{O}$  solution with a  $\text{DMSO-}d_6$  capillary tube insert ( $= 0$  ppm).

The recorded spectra were evaluated using MestReNova's NMR software and the DN values were assigned to the ILs by using a linear calibration line consisting of values for 16 different organic solvents as used in previous literature, the calibration line had a fit coefficient of around 0.95.<sup>17</sup>

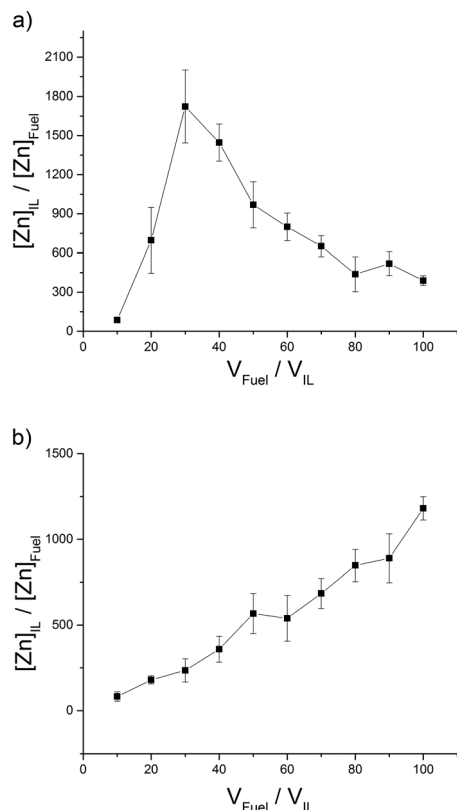


Fig. 3 ILs with intermediate distribution (I) of  $\text{Zn}^{2+}$  into the IL phase; (a)  $[(\text{CH}_3)_2\text{NH}_2][[(\text{CH}_3)_2\text{NCOO}]$  (b)  $[\text{C}_8\text{C}_1\text{im}]\text{Cl}$ .

### Kamlet–Taft measurements

Dye solutions of Reichardt's dye 30 (0.9 mM), *N,N*-diethyl-4-nitroaniline (0.6 mM), and 4-nitroaniline (0.7 mM) were freshly prepared in dichloromethane (DCM). The appropriate volume of dye for the ionic liquids was then determined in 1 mL of DCM to give an absorbance value within the range of 0.5–1.0.

The ionic liquids (1 mL), in round bottomed flasks, were dried *in vacuo* overnight at 60 °C prior to each measurement. The appropriate volume of freshly made dye was added the flask before the DCM was removed at 60 °C under vacuum for 1 h. The sample was allowed to cool and the UV-vis spectrum of each sample measured at 25 °C on a Perkin-Elmer Lambda 25 (200–1100 nm). The regression used in the determination of the Kamlet Taft parameters was calculated from a previous publication.<sup>18</sup>

### Density measurements

All samples were dried *in vacuo* prior to use and density measurements were carried out on a LiquiPhysics™ DM40 density metre at 25 °C and repeated three times to give an average result. The error associated with the measurement has been given as  $\pm 0.001 \text{ g cm}^{-3}$  by the manufacturer. A small amount (1–2 mL) of the sample was placed into the clean, dry, sample U tube of the instrument using a syringe. It was ensured that the sample tube was completely filled and that

no gas bubbles were present. After the temperature equilibrium has been reached, and the instrument displayed a steady reading to four significant figures, the density was recorded.

### Viscosity measurements

Viscosity measurements were determined at 298.15 K using an AR2000 rheometer (TA Instruments) which was fully calibrated prior to loading the sample. The measurements were recorded under an inert atmosphere using a truncated 40 mm 2° steel cone.

## Results and discussion

The fundamental design for this study required the selection of ionic liquids to provide suitable candidates for the application in addition to deriving the underlying mechanisms in the IL extraction of  $\text{Zn}^{2+}$  and  $\text{Cu}^{2+}$  from *n*-hexadecane. A variation of ILs, with unique physical properties, were synthesised to extract  $\text{Zn}^{2+}$  and  $\text{Cu}^{2+}$  ions from *n*-hexadecane. The ILs were selected to possess desirable characteristics such as low volatility and high thermal stability.<sup>19</sup> In previous research they have illustrated good extractability for metals from various media,<sup>20–22</sup> and due to their polarity are immiscible with hydrocarbons.<sup>23</sup> To provide an in-depth understanding of the system behaviour we included an IL with only CHNO atoms, in addition to ILs containing elements such as sulfur and phosphorus. In this application, it is suggested that the majority of ILs would decompose when exposed to the temperature conditions found in diesel engines, these decomposition products would then combust or vaporize.

After analysis of the fuel phase (post-extraction) we found that the ILs used had negligible solubility within the fuel phase to the level of being undetectable *via*  $^1\text{H}$  NMR or mass spectrometry. Solubility of the fuel in the IL was not investigated due to the IL being used as an extraction medium. To determine the properties of the ILs that are desired (and required) for this application anions were selected to give variety in their possible interactions with the  $\text{Zn}^{2+}$  and  $\text{Cu}^{2+}$  ions. We postulated that this proceeds *via* the IL extracting the zinc and copper directly from the fuel phase in a biphasic extraction. The sulfate, phosphate and acetate anions were selected because of being known for strongly interacting with metals through the formation of chelated complexes. It has been identified that sulfur is not suitable as a fuel additive<sup>24</sup> and the choice of the ILs with sulfur containing anions was purely for fundamental scientific purposes in order to gain understanding of the underlying chemical interactions controlling the extraction.

### Extraction experiments

Fig. 2–6 demonstrate that the ILs (Fig. 1) are highly successful in the biphasic extraction of  $\text{Zn}^{2+}$  and  $\text{Cu}^{2+}$  from our model fuels. The ILs were used in a biphasic extraction with an increasing fuel:IL ratio to isolate high performing

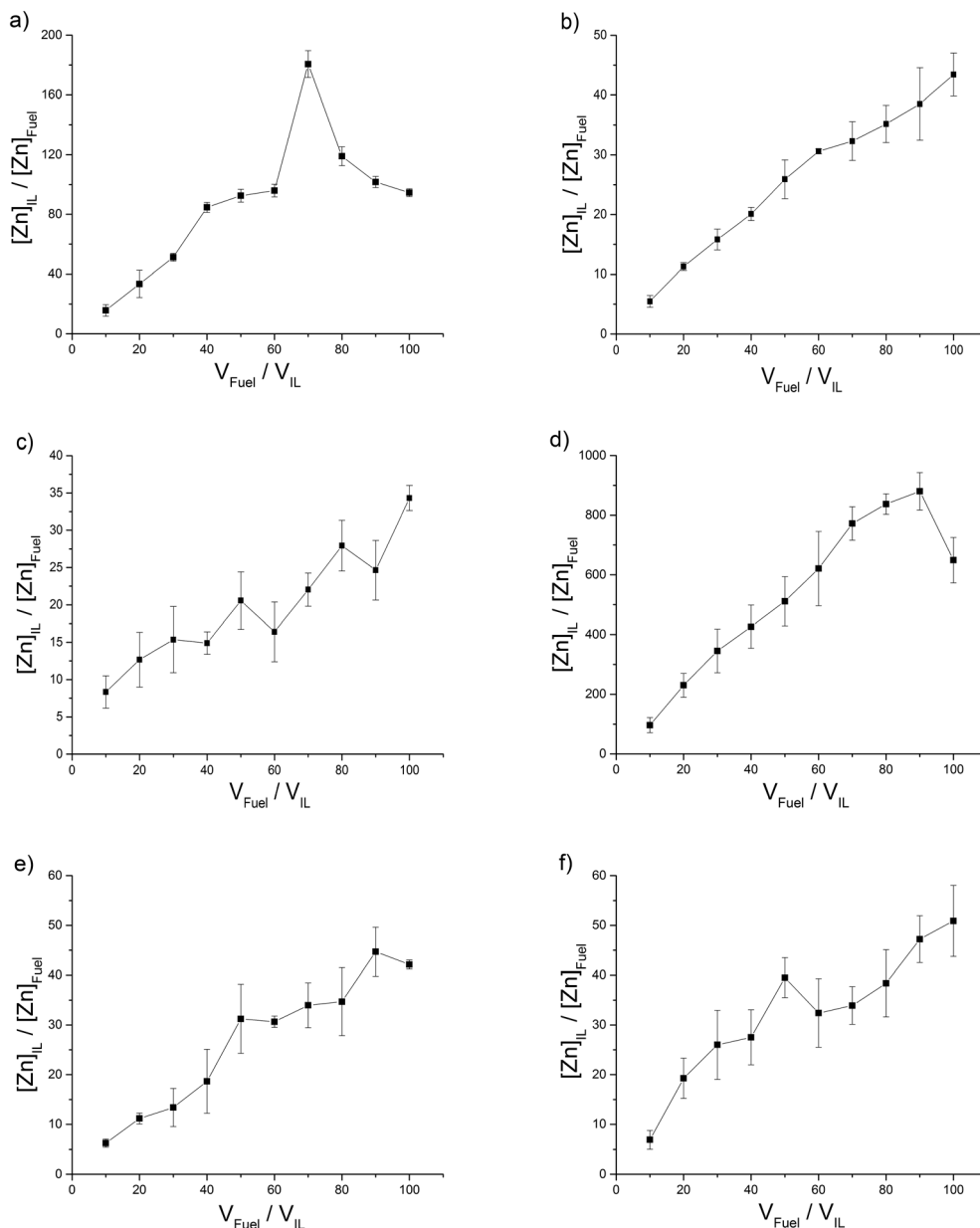


Fig. 4 ILs with a low distribution (L) of  $\text{Zn}^{2+}$  into the IL phase, (a)  $[\text{C}_4\text{C}_1\text{im}][\text{MeSO}_4]$ , (b)  $[\text{C}_4\text{C}_1\text{im}][\text{OTf}]$  (c)  $[\text{C}_4\text{C}_1\text{pyrr}][\text{OTf}]$ , (d)  $[\text{C}_8\text{C}_1\text{im}][\text{OTf}]$  and (e)  $[\text{C}_4\text{C}_1\text{im}][\text{N}(\text{Tf})_2]$  (f)  $[\text{C}_4\text{C}_1\text{pyrr}][\text{N}(\text{Tf})_2]$ .

candidates for further study. For example,  $[\text{C}_4\text{C}_1\text{im}][\text{OAc}]$  can extract 98.96% of the zinc present in the model fuel at a 100:1 fuel:IL ratio, and would ideally be suited to a fuel application due to it containing only CHNO atoms. The extractions were analysed, and the distribution coefficient for  $\text{Zn}^{2+}$  between the two phases calculated and plotted against the fuel:IL ratio. This provides an insight into the efficiency of the IL in the extraction of  $\text{Zn}^{2+}$  and  $\text{Cu}^{2+}$  from *n*-hexadecane.  $[\text{C}_4\text{C}_1\text{im}][\text{Me}_2\text{PO}_4]$  in the extraction of  $\text{Zn}^{2+}$  is highly effective giving a distribution coefficient of up to 8294 (fuel:IL ratio of 70:1) but due to the anion containing a phosphorus atom the IL's suitability is reduced.  $[\text{C}_4\text{C}_1\text{im}][\text{S}_2\text{CN}(\text{C}_2\text{H}_5)_2]$  and  $[\text{C}_4\text{C}_1\text{im}][\text{OAc}]$  are capable of high distribution coefficients which generally increase with increasing fuel loadings

whereas  $[\text{C}_4\text{C}_1\text{im}][\text{Me}_2\text{PO}_4]$  provides an optimal range in which the distribution of  $\text{Zn}^{2+}$  into the IL is greatest (50:1, 60:1, 70:1). High distribution coefficients (H) have been classified as those reaching above 2000 for  $\text{Zn}^{2+}$  (Fig. 2). The distribution maximum distribution coefficient for  $[\text{C}_4\text{C}_1\text{im}][\text{Me}_2\text{PO}_4]$  translates to an extraction of 99.2% of  $\text{Zn}^{2+}$  from the model fuel into the IL phase (Table E3†). It would be expected that the distribution coefficient would decrease with an increasing model fuel to IL ratio due to the volume of ionic liquid remaining constant and the model fuel increasing thus providing a greater amount of  $\text{Zn}^{2+}$  to extract. This is not the case for ILs such as  $[\text{C}_8\text{C}_1\text{im}]\text{Cl}$  which perform better at higher model fuel loading. The ILs  $[(\text{CH}_3)_2\text{NH}_2][(\text{CH}_3)_2\text{NCOO}]$  and  $[\text{C}_8\text{C}_1\text{im}]\text{Cl}$  give an intermediate distribution



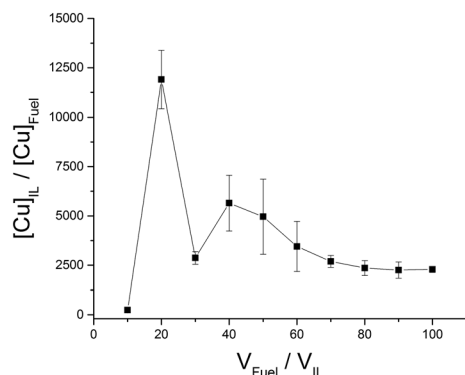


Fig. 5 ILs with high distribution of  $\text{Cu}^{2+}$  into the IL phase;  $[\text{C}_4\text{C}_1\text{im}][\text{OAc}]$ .

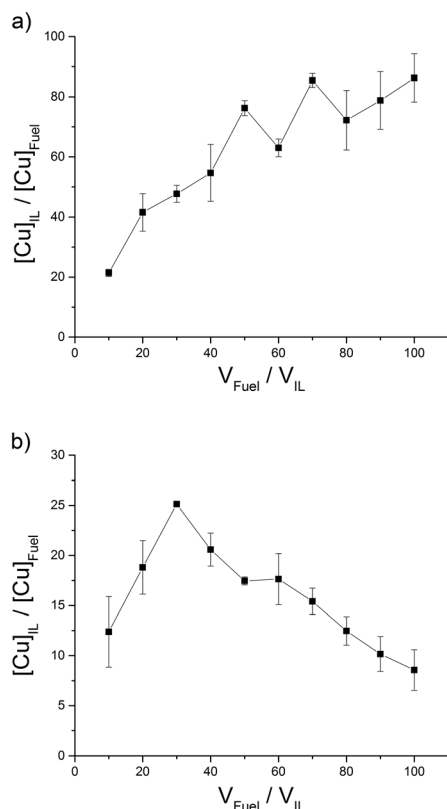


Fig. 6 ILs with a low distribution of  $\text{Cu}^{2+}$  into the IL phase, (a)  $[\text{C}_4\text{C}_1\text{im}][\text{MePO}_4]$ , (b)  $[(\text{CH}_3)_2\text{NH}_2][(\text{CH}_3)_2\text{NCOO}]$ .

coefficient (I) (Fig. 3) which we have classified as having a peak distribution coefficient reaching between 1000–2000 for  $\text{Zn}^{2+}$ . Distribution of  $\text{Zn}^{2+}$  into  $[(\text{CH}_3)_2\text{NH}_2][(\text{CH}_3)_2\text{NCOO}]$  increases with the volume of model fuel up to 1722 (fuel:IL ratio of 30:1) and then decreases dramatically with further increased fuel:IL volume ratio. The distribution of  $\text{Zn}^{2+}$  into  $[\text{C}_8\text{C}_1\text{im}]\text{Cl}$  gradually increases when the fuel:IL volume ratio is increased. We have classified ILs with a peak distribution coefficient below 1000 as low (L) extractors (Fig. 4). The  $[\text{N}(\text{Tf})_2]^-$  and  $[\text{OTf}]^-$  anion based ILs give a low distribution ef-

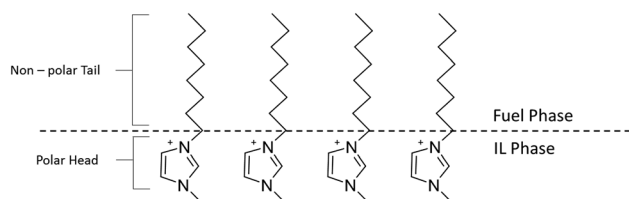


Fig. 7 Suggested arrangement of the octylimidazolium cation at the IL fuel interface.

iciency in the extraction of zinc which also increases with increasing volume of model fuel. One explanation for an increasing distribution coefficient could be that with increasing volume of model fuel the total amount of the ionic liquid lost into the model fuel could increase during the vortex mixing of the extractions. Another explanation is that the saturation of the IL is not reached and the increased volume of model fuel provides an increased number of ions and thus an (apparent) increased distribution coefficient. For these ILs the low distribution coefficient is likely due to the fluorine groups which are electron withdrawing, decreasing the interaction between the anion and positively charged metal. From the three  $[\text{OTf}]^-$  anion based ILs,  $[\text{C}_8\text{C}_1\text{im}][\text{OTf}]$  provides the largest peak distribution coefficient. An explanation for this could be the increased aggregation of the two phases caused by the long alkyl chain of the octylimidazolium cation. The long alkyl chain (non-polar tail) would have a higher affinity for the fuel phase and the polar head would have a higher affinity for the IL phase (Fig. 7).

The octylimidazolium ILs therefore act as a surfactant lowering surface tension between the phases and this would likely lead to an increased extraction.  $[\text{C}_4\text{C}_1\text{im}][\text{OAc}]$  and  $[\text{C}_4\text{C}_1\text{im}][\text{MePO}_4]$  were also tested in the removal of  $\text{Cu}^{2+}$  (Fig. 5 and 6a) from fuel due to their exceptional ability in the extraction of  $\text{Zn}^{2+}$  (Fig. 2 and c) and were expected to extract in the same way due to both metal complexes containing  $\text{M}^{2+}$  species.  $[\text{C}_4\text{C}_1\text{im}][\text{OAc}]$  in a similar fashion to  $\text{Zn}^{2+}$ , extracts  $\text{Cu}^{2+}$  with a high distribution giving a maximum distribution coefficient of 11 908 (Fig. 5). The low distribution of  $\text{Cu}^{2+}$  at 10:1 fuel:IL ratio would be expected due to the model fuel sample volume being small and thus close to the interface which could contain the metal.

$[(\text{CH}_3)_2\text{NH}_2][(\text{CH}_3)_2\text{NCOO}]$  was also used in addition these two ILs as it is a ready-made and cost effective IL containing only CHNO atoms.  $[\text{C}_4\text{C}_1\text{im}][\text{MePO}_4]$  and  $[(\text{CH}_3)_2\text{NH}_2][(\text{CH}_3)_2\text{NCOO}]$  both, compared to  $\text{Zn}^{2+}$ , give low distribution coefficients in the removal of  $\text{Cu}^{2+}$  (Fig. 6). This could also be due to the composition of the metal complexes in *n*-hexadecane since the peak distribution coefficient in the extraction of  $\text{Zn}^{2+}$  is greater than in  $\text{Cu}^{2+}$  for all ILs. The acetylacetonate ligand of  $\text{Cu}(\text{acac})_2$  is known to be a rather strong chelating agent.<sup>25</sup> This could affect the ability of the ILs to preferentially chelate to the metals. The same hierarchy system and values that was utilised for  $\text{Zn}^{2+}$  was used for  $\text{Cu}^{2+}$  *i.e.* high (H), intermediate (I) and low (L).

## IL characterisation

$^{23}\text{Na}$  NMR determined donor numbers (electron donating ability) and Kamlet–Taft data was gathered for each IL giving hydrogen-bond acidity/basicity ( $\alpha/\beta$ ) and dipolarity/polarizability effect ( $\pi^*$ ) values. Mechanisms were then derived for each of the extractions for each IL *via* comparison of the data. The donor number, DN, (defined by  $^{23}\text{Na}$  NMR) of the ILs was used in this study to define the Lewis basicity of the ILs. This is a term previously used to display and quantify solvent properties by Victor Gutmann.<sup>26</sup> He demonstrated that donor number could be used as a quantitative measure for the ability of the solvent to donate electron pairs to acceptors. Information on the donor number of ILs in this study allowed an estimation/determination of the strength of the interactions between the ILs anions and the dissolved zinc and copper ions in the model fuels. To provide a comparison of the extraction data and donor number the ranking system, high (H), intermediate (I) and low (L) was used in the extraction of  $\text{Zn}^{2+}$  and  $\text{Cu}^{2+}$  from *n*-hexadecane (Table 2). Due to the  $[\text{HSO}_4^-]$  anion based ILs giving erratic readings throughout the extraction experiments their characterisation will be displayed but will not be used in further discussion. The ILs were ordered in terms of their DN (Table 1) and it is clear to see that the ILs with a higher ability to extract  $\text{Zn}^{2+}$  have a larger DN with a discrepancy for the  $[(\text{CH}_3)_2\text{NH}_2][(\text{CH}_3)_2\text{NCOO}]$  which provides only an intermediate extraction ability but a relatively high DN. This difference is likely caused by the physical parameters of the system such as viscosity or density. For  $\text{Cu}^{2+}$  extraction the ILs were ordered in terms of their DN but the trend is not as clear as  $[\text{C}_4\text{C}_1\text{im}][\text{OAc}]$  has a high ability to extract  $\text{Cu}^{2+}$  but has the lowest DN whilst the other two ILs give a low extraction in comparison and have high DN (Table 3).

This could be explained again by the composition of the metal complex ( $\text{Cu}(\text{acac})_2$ ) in *n*-hexadecane. To further explain the relationship between the extraction of  $\text{Zn}^{2+}/\text{Cu}^{2+}$  and the ILs, Kamlet–Taft (KT) solvent parameters were determined (Table 4). DN displays the effect of the whole but KT allows comparisons to be drawn between the individual component ions of the IL. Using solvachromatic dyes KT data was gathered for each IL to determine their hydrogen-bond acidity/basicity ( $\alpha/\beta$ ) and dipolarity/polarizability ( $\pi^*$ ) effects which explains the ways that the solvents interact with solutes. Kamlet–Taft solvent descriptors have been used in ILs for a number of applications such as explaining their reactivity with anionic nucleophiles<sup>27</sup> and predicting how ILs work in catalysis.<sup>28</sup> These are capable of capturing the complexity of interactions that give rise to a solvent's overall polarity. The multi-parameter polarity scales are based upon linear solvation energy relationships (eqn (1)) composed of the complementary scales.<sup>18</sup>

$$(\text{XYZ}) = (\text{XYZ})_0 + a\alpha + b\beta + s\pi^* \quad (1)$$

$\pi^*$  is the value that most resembles ‘polarity’ in the absence of any hydrogen bonding effects. The values recorded are relatively high in comparison with most non-aqueous mo-

**Table 1**  $^{23}\text{Na}$  NMR chemical shift data and determined donor numbers

| Ionic liquid   | DN [kcal mol <sup>-1</sup> ] (ref.) | $^{23}\text{Na}$ chemical shift [ppm] |
|--|-------------------------------------|---------------------------------------|
| $[\text{C}_4\text{C}_1\text{im}][\text{N}(\text{Tf})_2]$                       | 9.9 (10.2) <sup>17</sup>            | -10.86                                |
| $[\text{C}_4\text{C}_1\text{im}][\text{OTf}]$                                  | 19.8                                | -6.17                                 |
| $[\text{C}_4\text{C}_1\text{im}][\text{MeSO}_4]$                               | 19.6                                | -6.25                                 |
| $[\text{C}_4\text{C}_1\text{im}][\text{Me}_2\text{PO}_4]$                      | 28.6                                | -1.98                                 |
| $[\text{C}_4\text{C}_1\text{im}][\text{HSO}_4]$                                | 13.6                                | -9.11                                 |
| $[\text{C}_4\text{C}_1\text{im}][\text{OAc}]$                                  | 21.3                                | -5.43                                 |
| $[\text{C}_4\text{C}_1\text{im}][\text{S}_2\text{CN}(\text{C}_2\text{H}_5)_2]$ | 32.2                                | -0.28                                 |
| $[\text{C}_4\text{C}_1\text{pyrr}][\text{N}(\text{Tf})_2]$                     | 7.4                                 | -12.01                                |
| $[\text{C}_4\text{C}_1\text{pyrr}][\text{OTf}]$                                | 16.4                                | -7.74                                 |
| $[\text{C}_8\text{C}_1\text{im}]\text{Cl}$                                     | 70.0 (69.2) <sup>17</sup>           | 17.71                                 |
| $[\text{C}_8\text{C}_1\text{im}][\text{OTf}]$                                  | 18.5 (18.6) <sup>17</sup>           | -6.75                                 |
| $[\text{C}_8\text{C}_1\text{im}][\text{HSO}_4]$                                | 19.4                                | -6.35                                 |

**Table 2** Hierarchy of ILs for this study in the ability to extract  $\text{Zn}^{2+}$  from *n*-hexadecane based on donor number

| Ionic liquid   | DN [kcal mol <sup>-1</sup> ] | Extractability ranking ( $\text{Zn}^{2+}$ ) |
|--|------------------------------|---|
| $[\text{C}_4\text{C}_1\text{im}][\text{S}_2\text{CN}(\text{C}_2\text{H}_5)_2]$ | 32.2                         | H   |
| $[\text{C}_4\text{C}_1\text{im}][\text{Me}_2\text{PO}_4]$                      | 28.6                         | H   |
| $[(\text{CH}_3)_2\text{NH}_2][(\text{CH}_3)_2\text{NCOO}]$                     | 24.6                         | I   |
| $[\text{C}_4\text{C}_1\text{im}][\text{OAc}]$                                  | 21.3                         | H   |
| $[\text{C}_4\text{C}_1\text{im}][\text{OTf}]$                                  | 19.8                         | L   |
| $[\text{C}_4\text{C}_1\text{im}][\text{MeSO}_4]$                               | 19.6                         | L   |
| $[\text{C}_8\text{C}_1\text{im}][\text{OTf}]$                                  | 18.5                         | L   |
| $[\text{C}_4\text{C}_1\text{pyrr}][\text{OTf}]$                                | 16.4                         | L   |
| $[\text{C}_4\text{C}_1\text{im}][\text{N}(\text{Tf})_2]$                       | 9.9                          | L   |
| $[\text{C}_4\text{C}_1\text{pyrr}][\text{N}(\text{Tf})_2]$                     | 7.4                          | L   |

**Table 3** Hierarchy of ILs for this study in the ability to extract  $\text{Cu}^{2+}$  from *n*-hexadecane based on donor number

| Ionic liquid   | DN [kcal mol <sup>-1</sup> ] | Extractability ranking ( $\text{Cu}^{2+}$ ) |
|--|------------------------------|---|
| $[\text{C}_4\text{C}_1\text{im}][\text{Me}_2\text{PO}_4]$  | 28.6                         | L   |
| $[(\text{CH}_3)_2\text{NH}_2][(\text{CH}_3)_2\text{NCOO}]$ | 24.6                         | L   |
| $[\text{C}_4\text{C}_1\text{im}][\text{OAc}]$              | 21.3                         | H   |

**Table 4** Kamlet–Taft parameters determined for the ILs studied

| Ionic liquid   | $\alpha$ (ref.)           | $\beta$ (ref.)             | $\pi^*$ (ref.)            |
|--|---------------------------|----------------------------|---------------------------|
| $[\text{C}_4\text{C}_1\text{im}][\text{N}(\text{Tf})_2]$   | 0.65 (0.62) <sup>29</sup> | 0.24 (0.24) <sup>29</sup>  | 0.92 (0.98) <sup>29</sup> |
| $[\text{C}_4\text{C}_1\text{im}][\text{OTf}]$              | 0.65 (0.63) <sup>29</sup> | 0.50 (0.46) <sup>29</sup>  | 0.94 (1.01) <sup>29</sup> |
| $[\text{C}_4\text{C}_1\text{im}][\text{MeSO}_4]$           | 0.57 (0.53) <sup>18</sup> | 0.67 (0.66) <sup>18</sup>  | 1.02 (1.06) <sup>18</sup> |
| $[\text{C}_4\text{C}_1\text{im}][\text{Me}_2\text{PO}_4]$  | 0.48 (0.45) <sup>18</sup> | 1.13 (1.13) <sup>18</sup>  | 0.93 (0.98) <sup>18</sup> |
| $[\text{C}_4\text{C}_1\text{im}][\text{OAc}]$              | 0.60 (0.57) <sup>27</sup> | 1.26 (1.18) <sup>27</sup>  | 0.93 (0.89) <sup>27</sup> |
| $[\text{C}_4\text{C}_1\text{pyrr}][\text{N}(\text{Tf})_2]$ | 0.45 (0.73) <sup>30</sup> | 0.20 (-0.11) <sup>30</sup> | 0.90 (0.89) <sup>30</sup> |
| $[\text{C}_4\text{C}_1\text{pyrr}][\text{OTf}]$            | 0.44 (0.40) <sup>31</sup> | 0.47 (0.46) <sup>31</sup>  | 0.94 (1.02) <sup>31</sup> |
| $[\text{C}_8\text{C}_1\text{im}]\text{Cl}$                 | 0.47                      | 1.00                       | 0.94                      |
| $[\text{C}_8\text{C}_1\text{im}][\text{OTf}]$              | 0.65                      | 0.53                       | 0.91                      |
| Ethanol  | (0.86) <sup>32</sup>      | (0.75) <sup>32</sup>       | (0.54) <sup>32</sup>      |

molecular solvents but remain steady throughout the ILs used in this study. The  $\alpha$ -values are largely determined by the nature of the cation, with a smaller anion effect, and fall between 0.44–0.65. In this study, we were most interested in the  $\beta$ -values as this is related to the anion of the IL and could allow us to correlate the chelating ability of our IL anion towards zinc and copper ions. As is shown in Table 4 this is the value in which the main variation exists.

However, the data gave a large enough span to correlate the ability of the IL extraction towards zinc and copper ions from the hydrocarbon streams. To deliver a more in depth understanding of the extraction mechanism, the density and viscosity of the ILs were compared to the peak distribution coefficient for each IL within the volume ratio range (10:1–100:1) (Table 5). It appears that the extraction of  $\text{Zn}^{2+}$  relies on a combination of these factors in addition to DN. In general, the ILs which work best have a high DN, high viscosity and a low density. For example,  $[\text{C}_4\text{C}_1\text{im}][\text{OAc}]$  has a high electron donating ability (DN), a relatively low density enabling the  $\text{Zn}^{2+}$  ions to cross over into the IL phase, and high viscosity to allow time to chelate  $\text{Zn}^{2+}$  within the IL. This appears to be the ideal conditions to support the highest possible distribution into the IL phase but the trend is not so evident to suggest that these are the only factors involved.  $[\text{C}_4\text{C}_1\text{im}][\text{S}_2\text{CN}(\text{C}_2\text{H}_5)_2]$  gives the highest DN, an exceptionally high viscosity but in the extraction of  $\text{Zn}^{2+}$  does not perform as well even though the density is marginally higher than that of  $[\text{C}_4\text{C}_1\text{im}][\text{OAc}]$ . The decreased performance could be a result of the high viscosity hindering the crossover of  $\text{Zn}^{2+}$  in to IL phase. This is why we have to generalise the trend in terms of ILs which extract more have a high DN and viscosity with a low density.

### Non-random two-liquid equation (NRTL)

To finalise this study, the activity coefficients of the  $\text{Zn}^{2+}$  in the IL and *n*-hexadecane (diesel) phases were evaluated using the non-random two-liquid (NRTL) model.

This model has been shown to be useful for correlating experimental liquid–liquid equilibrium data of systems containing ILs.<sup>33</sup> The results from the extraction were fitted to the NRTL model (eqn (2)) where  $g$  is an intermolecular

pair energy and  $\alpha$  is a non-randomness factor (in this study found to be between 0.1–0.5). The mixture is considered to be an ideal solution (completely random) when the value of  $\alpha$  is 0. This non-randomness parameter enables the NRTL model to be applied to various binary and tertiary mixtures due to the additional degree of freedom that it offers.

$$\frac{g^E}{RT} = \chi_1\chi_2 \left[ \frac{\tau_{21}G_{21}}{\chi_1 + \chi_2 G_{21}} + \frac{\tau_{12}G_{12}}{\chi_1 G_{12} + \chi_2} \right] \quad (2)$$

$$\text{where } \tau_{12} = \frac{g_{12} - g_{22}}{RT}; \tau_{21} = \frac{g_{12} - g_{11}}{RT} \quad (3)$$

$$G_{12} = \exp(-\alpha_{12} \tau_{21}); G_{21} = \exp(-\alpha_{12} \tau_{21})$$

The configuration of the NRTL model was processed *via* mole fraction values calculated from the experimental data obtained from the ICP-OES. To draw a comparison, estimates against experimental mole fractions ( $W_i$ ) were plotted for  $\text{Zn}^{2+}$  in both *n*-hexadecane and the IL using the  $[\text{C}_4\text{C}_1\text{im}][\text{Me}_2\text{PO}_4]$   $\text{Zn}^{2+}$  extraction as an exemplar (see ESI† Fig. E3).

Similarly, all ILs showed a good correlation for  $\text{Zn}^{2+}$  and  $\text{Cu}^{2+}$ .  $\tau$  values calculated *via* the model were compared with  $\tau$  values calculated from the extraction data to ensure that the NRTL model was in line with the experimental data (Fig. 8).  $[\text{C}_4\text{C}_1\text{im}][\text{S}_2\text{CN}(\text{C}_2\text{H}_5)_2]$  was removed from Fig. 8b and  $[\text{C}_4\text{C}_1\text{im}][\text{Me}_2\text{PO}_4]$  was removed from both Fig. 8a and b to provide a clear trend between the  $\tau$  values (complete table of  $\tau$  values can be found in the ESI†). A linear regression with DN was used as we trust that this factor provides information on the whole liquid opposed to  $\beta$  which provides data relating to the anion of the ionic liquid.  $[\text{C}_8\text{C}_1\text{im}]\text{Cl}$  was removed from the DN work in this section due to having an exceptionally high DN in comparison to other ILs. To carry out the liquid–liquid equilibrium calculation, phase compositions were obtained by solving an isothermal liquid–liquid flash at a given temperature and pressure.

The flash calculation consists of the following system of equations.

Equilibrium equation:

$$x_i^{L1} \gamma_i^{L1} - x_i^{L2} \gamma_i^{L2} = 0, i = 1, N_c \quad (4)$$

Equation of summation:

$$\sum_i x_i = 1 \quad (5)$$

where,  $x_i$  is the amount of component  $i$  in the mixture;  $x_i^{L1}$  is the amount of component  $i$  in liquid phase L1;  $x_i^{L2}$  is the amount of component  $i$  in liquid phase L2; and  $N_c$  is the number of constituents of the liquid phases.

**Table 5** Peak distribution coefficient ( $P$ ), viscosity ( $\eta$ ), donor number DN and density ( $\rho$ ) for the studied ILs

| Ionic liquid   | Peak $P$<br>( $\text{Zn}^{2+}$ ) | DN<br>[kcal mol <sup>-1</sup> ] | $\eta$<br>[Pa s <sup>-1</sup> ] | $\rho$<br>[g cm <sup>-3</sup> ] |
|--|----------------------------------|---------------------------------|---------------------------------|---------------------------------|
| $[\text{C}_4\text{C}_1\text{im}][\text{S}_2\text{CN}(\text{C}_2\text{H}_5)_2]$ | 8081                             | 32.2                            | 2.39                            | 1.083                           |
| $[\text{C}_4\text{C}_1\text{im}][\text{Me}_2\text{PO}_4]$                      | 8294                             | 28.6                            | 0.13                            | 1.158                           |
| $[(\text{CH}_3)_2\text{NH}_2][(\text{CH}_3)_2\text{NCOO}]$                     | 1722                             | 24.6                            | 0.05                            | 1.050                           |
| $[\text{C}_4\text{C}_1\text{im}][\text{OAc}]$                                  | 13 061                           | 21.3                            | 0.16                            | 1.066                           |
| $[\text{C}_4\text{C}_1\text{im}][\text{OTf}]$                                  | 43.42                            | 19.8                            | 0.08                            | 1.295                           |
| $[\text{C}_4\text{C}_1\text{im}][\text{MeSO}_4]$                               | 180.61                           | 19.6                            | 0.09                            | 1.200                           |
| $[\text{C}_8\text{C}_1\text{im}][\text{OTf}]$                                  | 880.2                            | 18.5                            | 0.18                            | 1.201                           |
| $[\text{C}_4\text{C}_1\text{pyrr}][\text{OTf}]$                                | 34.32                            | 16.4                            | 0.13                            | 1.249                           |
| $[\text{C}_4\text{C}_1\text{im}][\text{N}(\text{Tf})_2]$                       | 44.70                            | 9.9                             | 0.04                            | 1.431                           |
| $[\text{C}_4\text{C}_1\text{pyrr}][\text{N}(\text{Tf})_2]$                     | 50.89                            | 7.4                             | 0.07                            | 1.394                           |



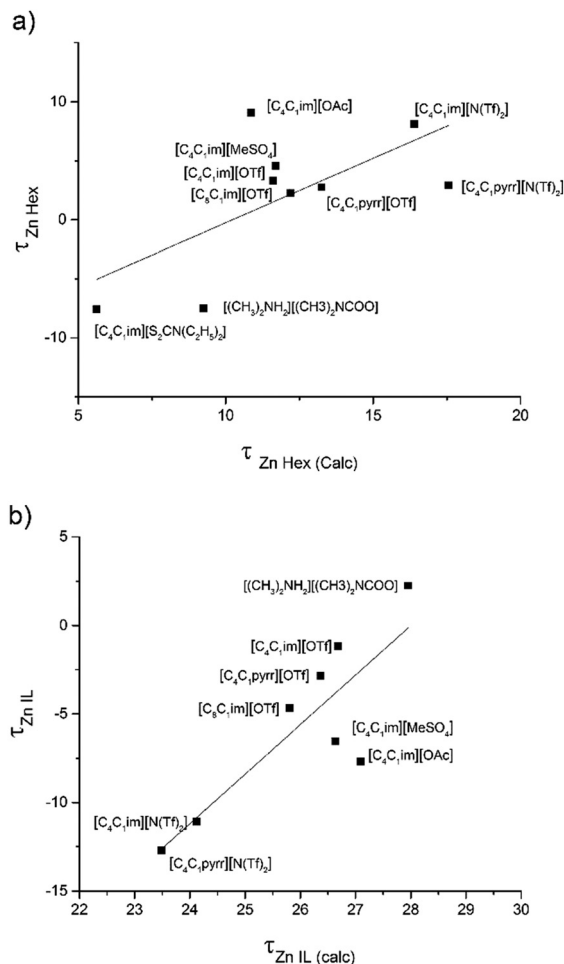


Fig. 8 Comparison of calculated (from experimental DN values) and NRTL model  $\tau$  parameters (a)  $\text{Zn}^{2+}$  in *n*-hexadecane and (b)  $\text{Zn}^{2+}$  in IL.

For a multicomponent system such as this, the activity coefficient of component *i* is given by the general expression:

$$\ln \gamma_i = \frac{\sum_j \tau_{ji} G_{ji} x_j}{\sum_j \tau_{ji} x_j} + \sum_j \frac{G_{ji} x_j}{\sum_k G_{kj} x_k} \left( \tau_{ij} - \frac{\sum_k \tau_{kj} G_{kj} x_k}{\sum_j \tau_{ji} G_{ji} x_j} \right) \quad (6)$$

With  $\ln G_{ij} = -\alpha_{ij} \tau_{ij}$ ,  $\alpha_{ij} = \alpha_{ji}$  and  $\tau_{ii} = 0$  where  $\tau_{ij}$  and  $\tau_{ji}$  are binary interaction parameters, and  $\alpha_{ij}$  is the non-randomness parameter. The non-randomness parameter enables the NRTL model to be applied to various binary and ternary mixtures because of the additional degree of freedom given by *ij*.

The correlation between DN and  $\tau$  values was analysed (Fig. 9) and displays the same trend as reported in our Na study,<sup>12</sup> displaying ILs with particular anions grouping into clusters. In this data, the line was used to guide the eye rather than a line of best fit. Generally, as DN increases the  $\tau$  parameter decreases for  $\text{Zn}^{2+}$  in *n*-hexadecane and increases for  $\text{Zn}^{2+}$  in the IL. This provides a general trend showing the

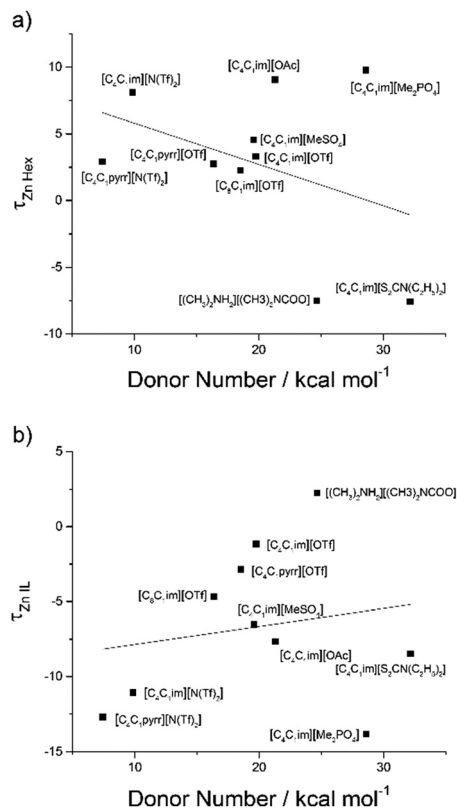


Fig. 9  $\tau$  vs. donor number (a)  $\text{Zn}^{2+}$  in *n*-hexadecane and (b)  $\text{Zn}^{2+}$  in IL.

anion effect and which phase is preferable for the Zn cations in the extraction system. This analysis demonstrates that the NRTL model could be used to predict the  $\text{Zn}^{2+}$  and potentially  $\text{Cu}^{2+}$  distribution into various ILs, or at least IL anion families, provided the  $\beta$  values (and DN and therefore  $\tau$ ) are known. As only three ILs were used in the extraction of  $\text{Cu}^{2+}$  a model has not yet been attempted and will be included in further research.

## Conclusions

Overall, a wide selection of ILs were synthesised and examined for their extraction efficiency in removal of zinc and copper ions from *n*-hexadecane based model diesel fuels at a concentration of 2 and 1 mg kg<sup>-1</sup> respectively. They have shown an array of trends in the extraction of  $\text{Zn}^{2+}$  and  $\text{Cu}^{2+}$  and show different distribution coefficients between them. We have extracted 99.3% of  $\text{Zn}^{2+}$  and 99.7% of  $\text{Cu}^{2+}$  at a 100 : 1 (fuel : IL) volume ratio using  $[\text{C}_4\text{C}_1\text{im}][\text{OAc}]$  as the best performing IL for the extraction of both metals. This is the most suitable IL from an industrial viewpoint due to high distribution coefficient, and suitable elemental make-up for a fuel application (CHNO). In addition to this, the ILs within the *n*-hexadecane were undetectable *via* NMR spectroscopy, and mass spectroscopy, thus all of the successful ILs in this study can be considered for an application in metal extraction from fuel. Minimal loss of IL to the *n*-hexadecane phase is also beneficial for industrial applications due to minimal

usage loss of the IL and hence negligible contamination of the processed fuel in addition to the possibility of recycling the IL.

The ability of each ionic liquid was determined *via* distribution coefficients for Zn<sup>2+</sup> and Cu<sup>2+</sup> into each IL over an increased volume of model fuel (10–100 mL). Factors affecting the extent of extraction were investigated *via* correlation with experimental solvent descriptors, providing a strong link between the ILs ability to extract zinc and copper with Kamlet-Taft's  $\beta$  values and <sup>23</sup>Na donor number. Application of the NRTL model to the experimental data determined  $\tau$  values for each of the IL showed some correlation to the DN and  $\beta$  values. All the data was taken into consideration when deducing a suitable extraction mechanism for the ILs. However, some of the ILs in this study gave a low distribution of zinc and copper into the IL phase which is thought to be caused by the low affinity of the anion towards zinc and copper in addition to the properties of the ILs themselves – density and viscosity.

## Conflicts of interest

There are no conflicts to declare.

## Acknowledgements

The authors gratefully acknowledge the help of Eduards Bakis for his valuable conversations, Dr Maria Teresa Mota Martinez for her assistance with computational modelling, EPSRC and Shell Global Solutions for the sponsorship of PJC.

## Notes and references

- J. Tang, S. Pischinger, U. Grütering and J. Keck, *MTZ Worldw.*, 2008, vol. 69, pp. 64–69.
- R. Caprotti and A. Breakspear, *SAE Tech. Pap. Ser.*, 2006, 2016-01-3359.
- M. Gee, *Personal Communication*, 2016.
- J. Reid, S. Cook and J. Barker, *SAE Int. J. Fuels Lubr.*, 2014, 7, 2014-01-1388.
- T. Welton, *Ionic Liquids in Synthesis*, Wiley, 2nd edn, 2007.
- J. P. Hallett and T. Welton, *Chem. Rev.*, 2011, 111, 3508–3576.
- N. V. Plechkova and K. R. Seddon, *Chem. Soc. Rev.*, 2008, 37, 123–150.
- T. D. Ho, C. Zhang, L. W. Hantao and J. L. Anderson, *Anal. Chem.*, 2014, 86, 262–285.
- H. Olivier-Bourbigou, L. Magna and D. Morvan, *Appl. Catal., A*, 2010, 373, 1–56.
- H. Passos, M. G. Freire and J. A. P. Coutinho, *Green Chem.*, 2014, 16, 4786–4815.
- B. Rodríguez-Cabo, H. Rodríguez, E. Rodil, A. Arce and A. Soto, *Fuel*, 2014, 117, 882–889.
- P. J. Corbett, A. J. S. McIntosh, M. Gee and J. P. Hallett, *Mol. Syst. Des. Eng.*, 2018, DOI: 10.1039/C7ME00110J.
- G. Hogarth, *Transition Metal Dithiocarbamates: 1978–2003 in Progress in Inorganic Chemistry*, ed. K. D. Karlin, John Wiley & Sons, Inc., Hoboken, NJ, USA, 2005, ch. 2, DOI: 10.1002/0471725587.
- K. B. Pandeya, R. Singh, P. K. Mathur and R. P. Singh, *Transition Met. Chem.*, 1986, 11, 347.
- R. H. Wendt and V. A. Fassel, *Anal. Chem.*, 1965, 37, 920–922.
- M. Thompson, J. N. Walsh, S. J. Walton and G. E. M. Hall, *Handbook of Inductively Coupled Plasma Spectrometry*, 1989.
- M. Schmeisser, P. Illner, R. Puchta, A. Zahl and R. Van Eldik, *Chem. - Eur. J.*, 2012, 18, 10969–10982.
- M. A. Ab Rani, A. Brant, L. Crowhurst, A. Dolan, M. Lui, N. H. Hassan, J. P. Hallett, P. A. Hunt, H. Niedermeyer, J. M. Perez-Arlandis, M. Schrems, T. Welton and R. Wilding, *Phys. Chem. Chem. Phys.*, 2011, 13, 16831–16840.
- Y. Meng, B. Liang and S. Tang, *Appl. Catal., A*, 2012, 439–440, 1–7.
- H. Luo, S. Dai and P. V. Bonnesen, *Anal. Chem.*, 2004, 76, 2773–2779.
- A. E. Visser, R. P. Swatloski, W. M. Reichert, R. Mayton, S. Sheff, A. Wierzbicki, J. H. Davis and R. D. Rogers, *Chem. Commun.*, 2001, 135–136.
- G.-T. Wei, Z. Yang and C.-J. Chen, *Anal. Chim. Acta*, 2003, 488, 183–192.
- H. Lü, W. Ren, H. Wang, Y. Wang, W. Chen and Z. Suo, *Appl. Catal., A*, 2013, 453, 376–382.
- J. C. Chow, *J. Air Waste Manage. Assoc.*, 2001, 51, 1258–1270.
- E. Lacote, B. Charleux and C. Coperet, *Chemistry of Organohybrids: Synthesis and Characterization of Functional Nano-Objects*, John Wiley & Sons, 2015.
- V. Gutmann, *Electrochim. Acta*, 1976, 21, 661–670.
- L. Crowhurst, R. Falcone, N. L. Lancaster, V. Llopis-Mestre and T. Welton, *J. Org. Chem.*, 2006, 71, 8847–8853.
- T. Welton, *Coord. Chem. Rev.*, 2004, 248, 2459–2477.
- C. Chiappe, C. S. Pomelli and S. Rajamani, *J. Phys. Chem. B*, 2011, 115, 9653–9661.
- N. D. Khupse and A. Kumar, *J. Phys. Chem. B*, 2010, 114, 376–381.
- G. Ranieri, J. P. Hallett and T. Welton, *Ind. Eng. Chem. Res.*, 2008, 47, 638–644.
- C. Reichardt, *Solvents and solvent effects in organic chemistry*, 2003.
- H. F. Hizaddin, M. K. Hadj-Kali, A. Ramalingam and M. A. Hashim, *Fluid Phase Equilib.*, 2015, 405, 55–67.